Supporting information

Natural killer cells induce distinct modes of cancer cell death: Discrimination, quantification and modulation of apoptosis, necrosis and mixed forms

Christian S. Backes[1], Kim S. Friedmann[1], Sebastian Mang[1], Arne Knörck[1], Markus Hoth[1]*, Carsten Kummerow[1]*

From the [1]Department of Biophysics, Center for Integrative Physiology and Molecular Medicine, School of Medicine, Saarland University, 66421 Homburg, Germany.

Running title: *NK cells induce distinct modes of cancer cell death*

* To whom correspondence should be addressed:

Carsten Kummerow, Biophysics, Center for Integrative Physiology and Molecular Medicine, Saarland University, 66421 Homburg, Germany;

carsten.kummerow@uks.eu; Tel. +49 6841 1616318; Fax. +49 6841 1616302.

Markus Hoth, Biophysics, Center for Integrative Physiology and Molecular Medicine, Saarland University, 66421 Homburg, Germany;

markus.hoth@uks.eu; Tel. +49 6841 1616303; Fax. +49 6841 1616302.

Key words: apoptosis, calcium, cancer, caspase, cellular immune response, cell death, imaging, immunology, natural killer cells (NK cells), necrosis

Supplementary Figures

Figure S1. Flow cytometry analysis of table target cell lines Jurkat pCasper and K562 pCasper.

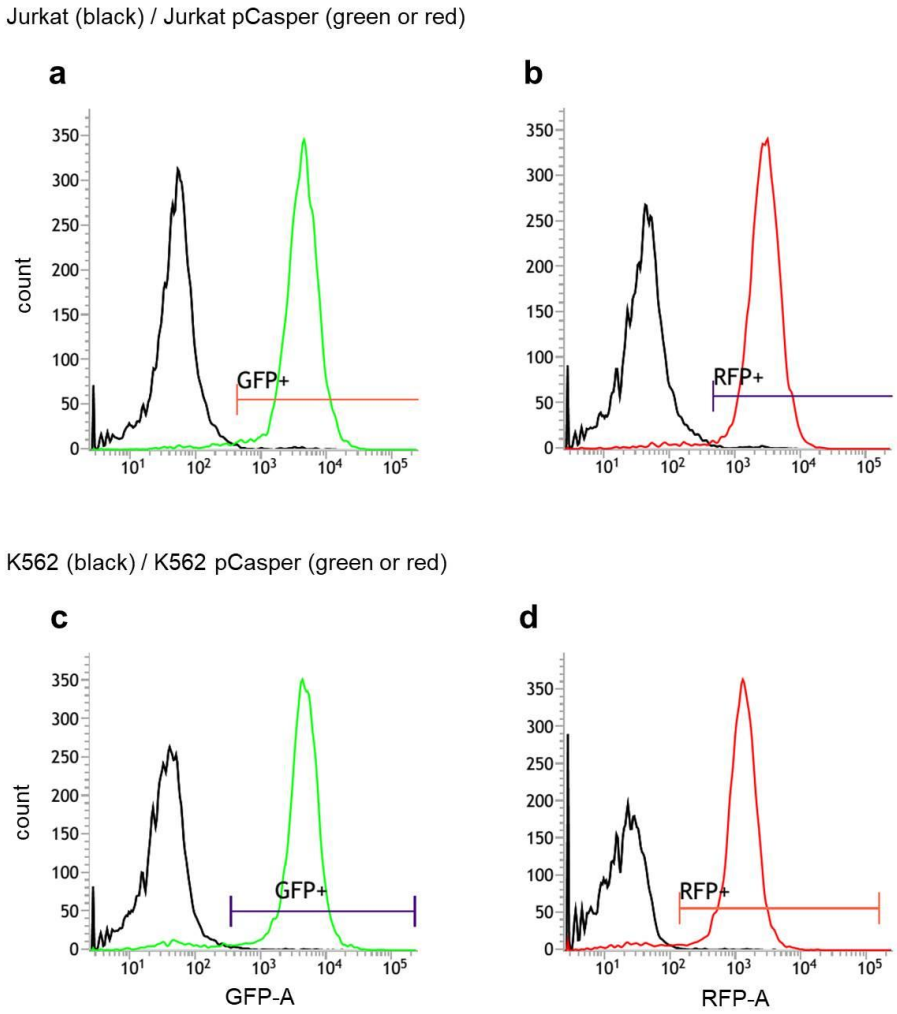

To check the quantity of fluorescent cells, both monoclonal, stable target cell lines (Jurkat pCasper and K562 pCasper) were analyzed by flow cytometry. Comparing them to the original cell lines (black), flow cytometry analysis confirmed, that in both cases > 93 % of Jurkat pCasper (*a*, *b*) or K562 pCasper (*c*, *d*) show a fluorescent signal in the green or red channel, respectively (green, red), indicating the expression of GFF and RFP.

Figure S2. **Analyzing Jurkat pCasper and K562 pCasper for CD95 expression using flow cytometry and qRT-PCR**.

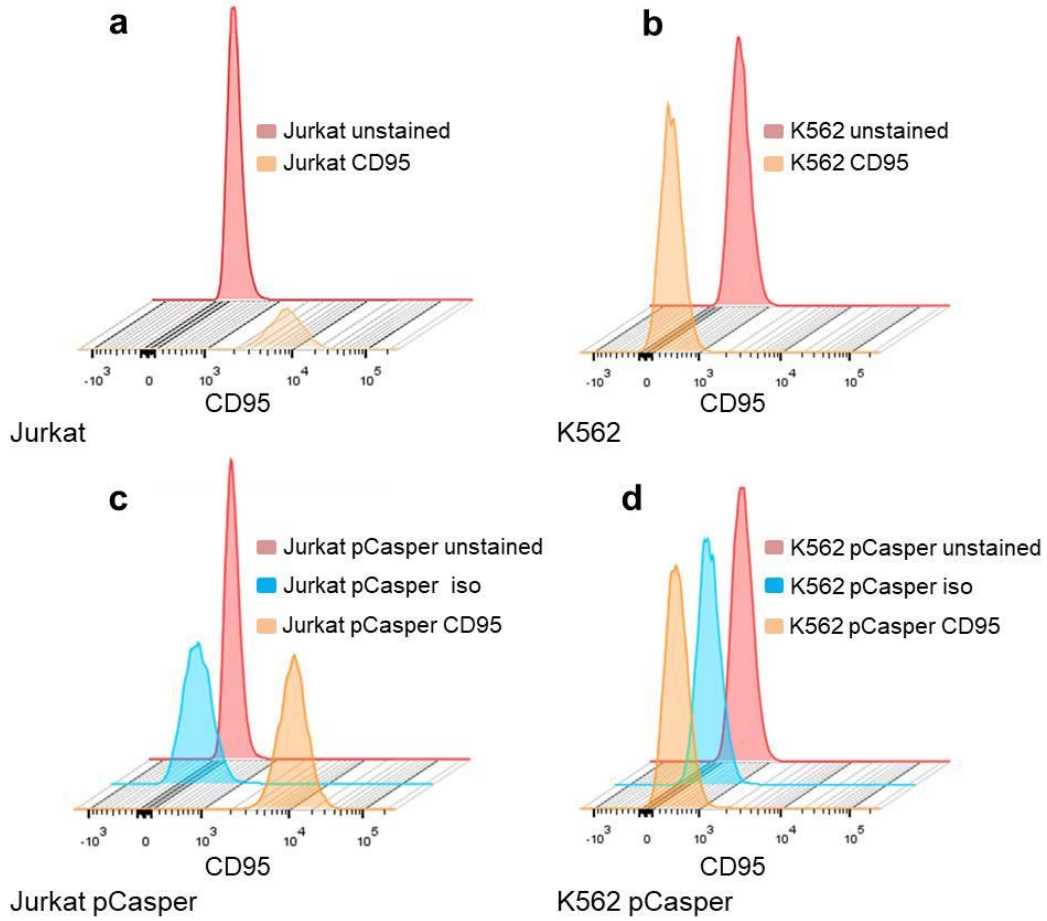

To check for CD95 expression of Jurkat pCasper and K562 pCasper cells, flow cytometry-analysis and qRT-PCR were performed. (*a*, *b*) Staining with anti-CD95 antibodies revealed that Jurkat E6-1 cells express CD95 (yellow) as previously shown by Caricchio et al. (Caricchio et al, 1998) whereas K562 cells do not express CD95 (yellow) as previously shown by Munker et al. (Munker et al, 1997). (*c*, *d*) Jurkat pCasper also express CD95 on the surface (yellow) compared to unstained cells or isotype control, whereas K562 pCasper cells (yellow) do not express CD95 compared to unstained cells or isotype control. Flow cytometry results were confirmed by qRT-PCR (see also Table S1).

Figure S3. **Lytic granules always accumulate at the immunological synapse if necrosis is induced in target cells by NK cells**.

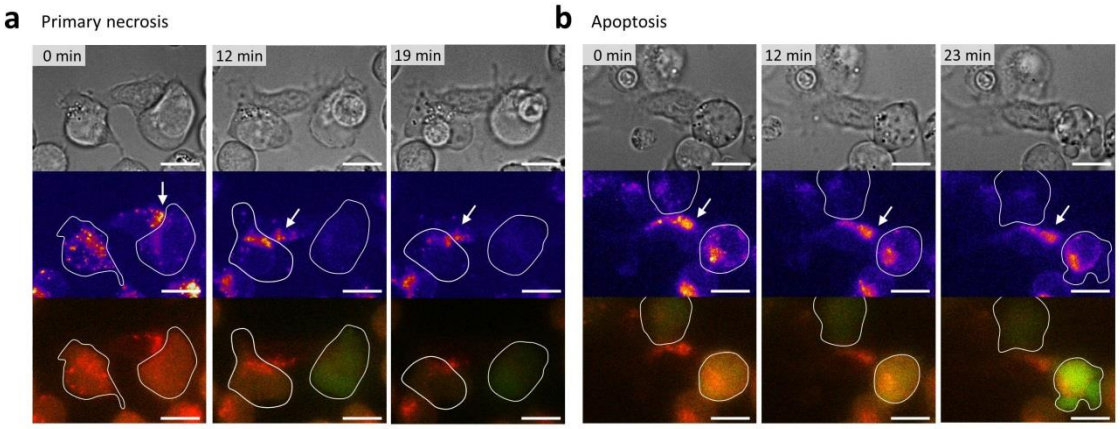

After pre-staining of NK lytic granules, 400 nM LysoTracker was added to the supernatant to counteract bleaching. Therefore target cell vesicles are also visible. Imaging data was generated via looped 2D and 3D time lapse imaging. For the looped protocol, brightfield pictures were acquired at the central focal plane in 2D at a 5 min interval using the Leica TIRF setup with a 63x oil immersion objective. GFP and FRET Signals were acquired likewise at 1 min intervals. Vesicle data was acquired as a z-stack of 42 frames and 350 nm step size covering the full volume of the target cell. The z-stacks were taken at 3.5 second intervals. Z-Stack is shown as maximum intensity projection (MIP), shown in Rainbow LUT color code.

Vesicles translocate as one coherent group in 10 out of 10 experiments, representative data is shown. (*a*) When NK cells induce necrosis, the vesicle group is always translocated to the NK-target cell contact site prior to target necrosis and lytic granules are always present at the contact site when the target cell loses membrane integrity (6 out of 6 of cases). The example shown is a representative example out of a dataset of 6 necrosis events. (*b*) Target cell apoptosis can occur without lytic granules being present near the NK cell – target cell contact site. In 4 out of 8 cases, lytic granules were not close to the contact site.

Figure S4. Comparing death plots by manual vs automated analysis for three different blood donors.

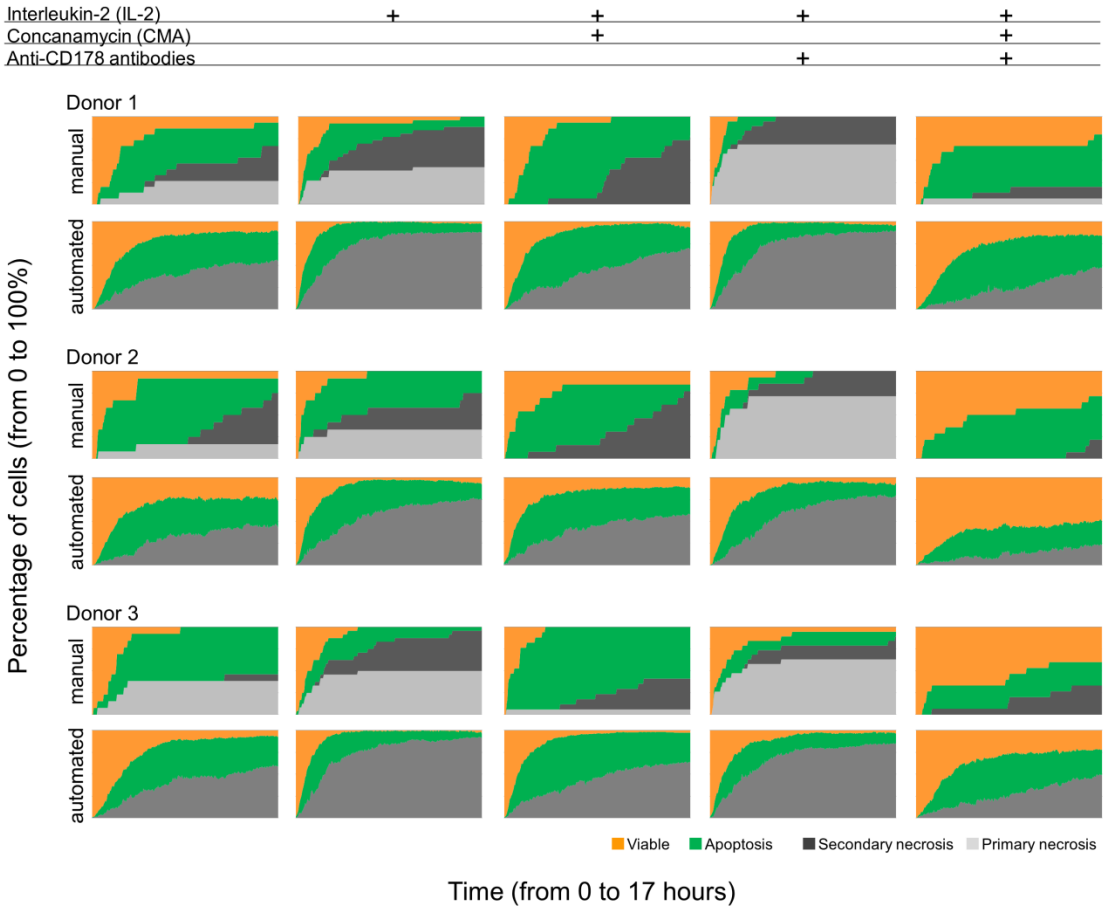

Experiments were performed exactly as described for Fig. 3 for three different blood donors. Manual analysis (upper panels) compared to automated analysis (lower panels) is compared for each blood donor. Cell numbers range from 15-20 for manual analysis and from 250-300 for automated analysis.

Figure S5. Caspase3-deficient MCF-7 cells can be killed via apoptosis by primary NK cells.

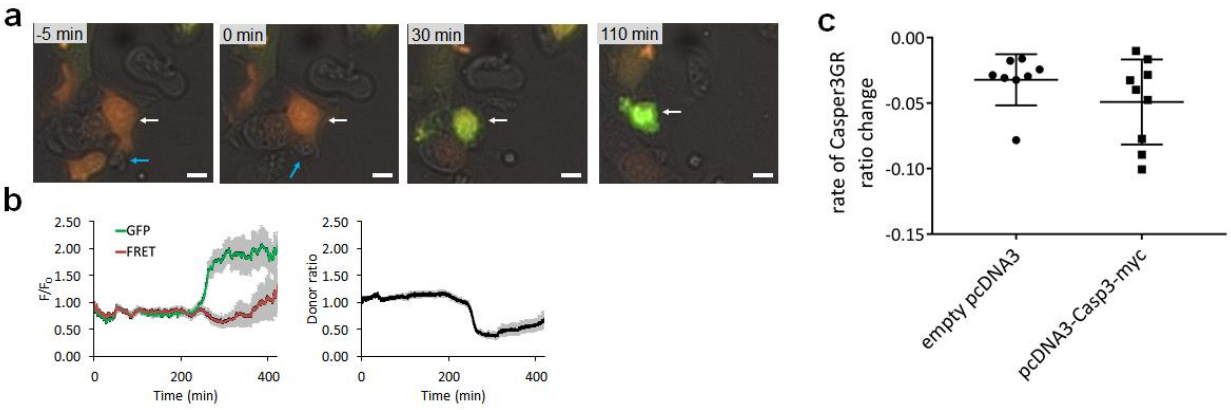

Caspase3-deficient MCF-7 cells were transfected with pCasper-GR construct. (*a*) Primary human NK cell (blue arrow) induce caspase dependent apoptosis in a pCasper-GR expressing MCF-7 cell (white arrow) indicated by the fluorescence change from red to green. (*b*) Average of 16 MCF-7 cells killed by NK cells. (*c*) Caspase-3 deficient MCF-7 cells and MCF-7 cells rescued with a caspase-3 coding vector (pcDNA3-Casp3-myc) were compared regarding the rate of the Casper-GR signal decline following NK cell contact. Scale bar is 10 µm.

Figure S6. **Characterization of the purified NK population**.

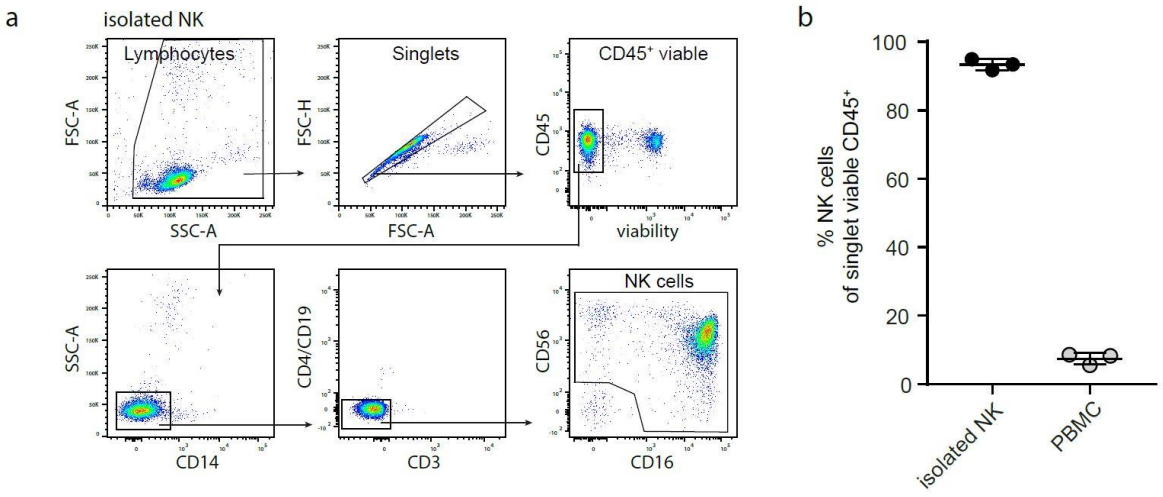

Cells were isolated from PBMC using the Dynabead® Untouched^{TM} NK cell isolation kit. Frequency of NK cells in the PBMC sample before isolation and purity after isolation were analyzed by flow cytometry. (*a*) Gating strategy shown for isolated NK cells of one representative donor. Lymphocytes were selected in a broad forward and side scatter gate. Doublet cells were excluded by forward area and height, before gating on $CD45^+$, live (amine reactive dye^-) cells. $CD3^+$, $CD4^+$, $CD14^+$, $CD19^+$ or SSC^{hi} cells were all excluded. (*b*) The purity of NK cells for three healthy donors (mean ± SD 93.3 ± 1.6 %) is shown as a percentage of singlet, viable, $CD45^+$ cells, in comparison to the frequency of NK cells within the PBMC sample (7.5 ± 1.7 %).

Figure S7. **FRET donor-ratio, correction factors**.

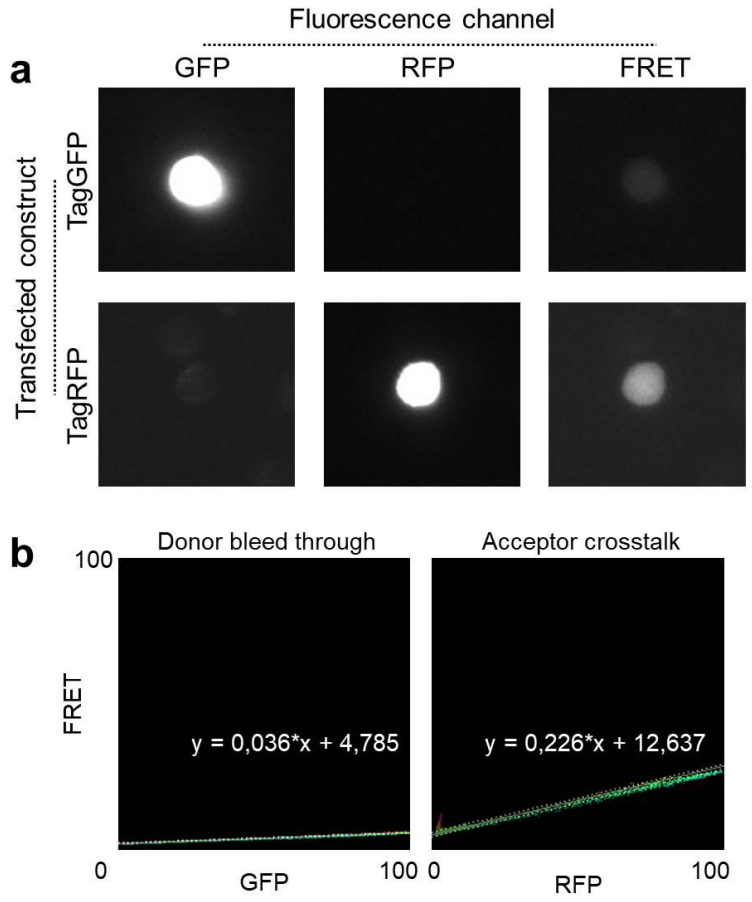

(*a*) To correctly quantify Casper-GR fluorescence, acceptor crosstalk and donor bleed-through were assessed (Youvan et al, 1997). TagGFP and TagRFP, were separately transfected into Jurkat E6-1 and for each transfection all emission channels were quantified. The percentage of crosstalk was determined for the given filter setting using identical illumination times and LED intensities with the Zeiss Cell observer (20x objective). Examples of one TagGFP and one TagRFP cell measured in the GFP, RFP and FRET channels are shown. (*b*) fluorescence intensities in the FRET channel were plotted against intensities in the TagGFP or TagRFP channel for each pixel from 5 cells, respectively. A linear equation was fitted to the data with Pearson correlation coefficients of 0.77 for donor bleed-through and 0.81 for acceptor crosstalk. The slope of the two fits reflects donor bleed-through to be 3.6 % and acceptor crosstalk to be 22.6 %. FRET signals were calculated by linear unmixing, using these correction factors.

Based on this, the intensity independent Youvan donor ratio (as for instance shown in Fig. 1*e*) was calculated by dividing the corrected FRET signal by the GFP signal.

Figure S8. **Donor ratio histograms and FRET histograms from automated analysis of target cell apoptosis and necrosis induced by NK cells**.

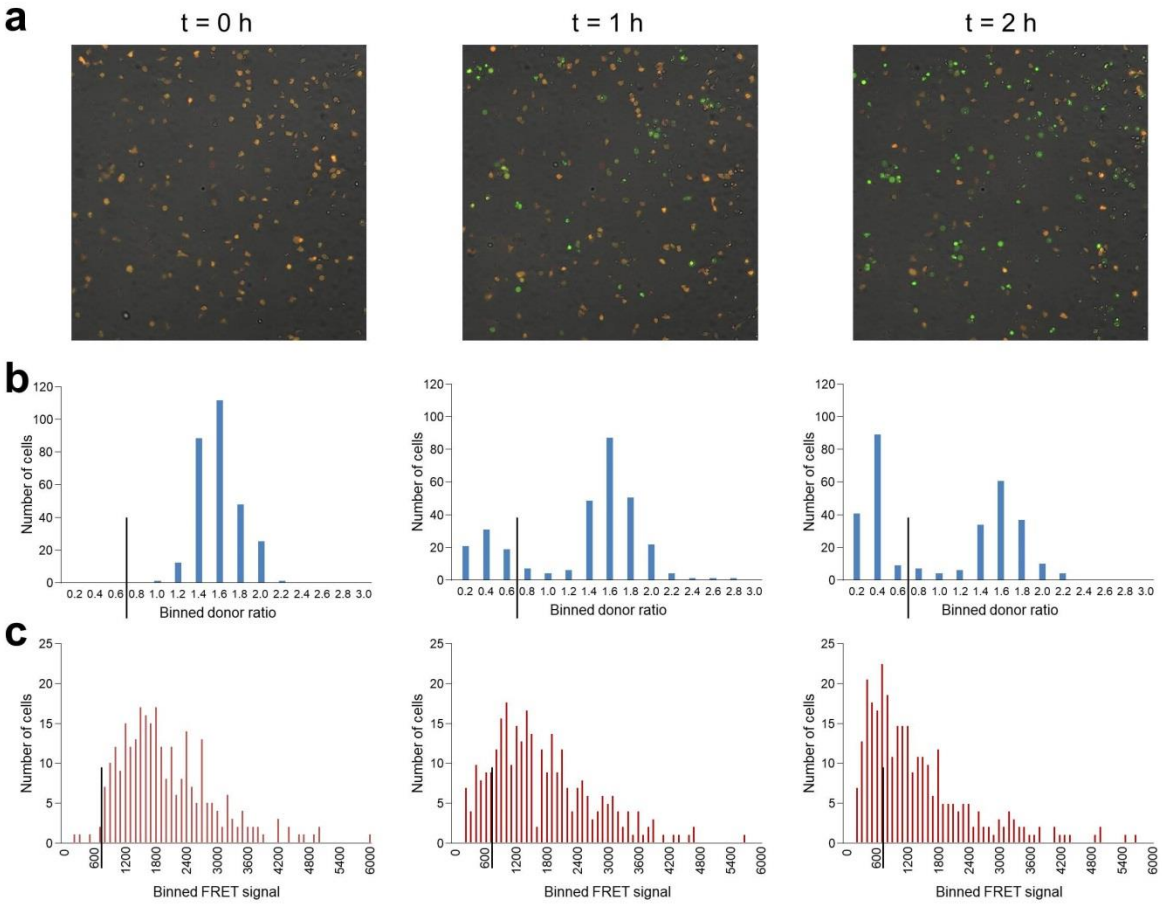

(*a*) Representatives images of Jurkat pCasper cells killed by NK cells. The frame at t = 0 hours was taken before NK cell killing of target cells had started. Conditions are similar as in Fig. 5*a-b*. Target cell killing was analyzed semi-automatically as described in the methods section. (*b*) A decrease of donor ratios was used to determine target cell apoptosis. Donor ratios of each target cell in the field were determined. Histograms of donor ratios are shown for three time points. At t = 0 h almost all cells are viable (orange). All donor ratios are higher than 0.6 which was set as a threshold to discriminate viable from apoptotic target cells. Over time an apoptotic population of targets is visible with donor ratios smaller than 0.6. (*b*) A decrease of FRET signals was used to determine target cell necrosis. FRET signals of each target cell in the field were determined. Histograms of FRET signals are shown for three time points. At t = 0 hours, FRET values of almost all cells are larger than 600 fluorescence units, which was thus used as a cutoff value for target cell necrosis.

Table S1. **qRT-PCR of CD95 compared to TBP and RNApol**.

	CD95 PP1/TBP	**CD95 PP1/RNAPol**	**CD95 PP2/TBP**	**CD95 PP2/RNAPol**
K562	0.000053	0.000075	0.000382	0.000539
K562 pCasper	0.000109	0.000148	0.000934	0.00127
Jurkat	0.1475	0.0866	1.0151	0.5964
Jurkat pCasper	0.1497	0.097	1.0588	0.6857

Values for two primer pairs against CD95 (PP1 and PP2) were normalized against two reference genes, TBP and RNApol (Wenning et al, 2011) and are shown as $2^{-\Delta Cq}$. The values clearly indicate that Jurkat E6-1 and Jurkat pCasper cells express CD95 mRNA whereas K562 and K562 pCasper cells do not. Flow cytometry (Fig. S2) and qRT-PCR indicate that CD95 expression was unaffected by the generation of the stably-transfected cell lines.

Video S1. **A single NK cells kills cancer cells by apoptosis or necrosis**. The video shows a single NK cells, which appears in the field of view at the beginning of the movie. This NK cell kills cancer cells by apoptosis (green fluorescence) or necrosis (loss of fluorescence). Compare Fig. 2*a* for details.

References for Supporting information

Caricchio R, Reap EA, Cohen PL (1998) Fas/Fas ligand interactions are involved in ultraviolet-B-induced human lymphocyte apoptosis. *Journal of immunology* 161: 241-251

Munker R, Marini F, Jiang S, Savary C, Owen-Schaub L, Andreeff M (1997) Expression of CD95(FAS) by gene transfer does not sensitize K562 to Fas-killing. *Hematology and cell therapy* 39: 75-78

Wenning AS, Neblung K, Strauss B, Wolfs MJ, Sappok A, Hoth M, Schwarz EC (2011) TRP expression pattern and the functional importance of TRPC3 in primary human T-cells. *Biochimica et biophysica acta* 1813: 412-423

Youvan DC, Silva C, Bylina E (1997) Calibration of fluorescence resonance energy transfer in microscopy using genetically engineered GFP derivatives on nickel chelating beads. . *Biotechnology* 3: 1-18